

Review

Water Depollution and Photo-Detoxification by Means of TiO₂: Fluoroquinolone Antibiotics as a Case Study

Luca Pretali, Federica Maraschi, Alice Cantalupi, Angelo Albini and Michela Sturini * 

Department of Chemistry, University of Pavia, Viale Taramelli 12, 27100 Pavia, Italy; luca.pretali@gmail.com (L.P.); federica.maraschi@unipv.it (F.M.); alice.cantalupi01@universitadipavia.it (A.C.); angelo.albini@unipv.it (A.A.)

* Correspondence: michela.sturini@unipv.it; Tel.: +39-0382-98737

Received: 24 March 2020; Accepted: 1 June 2020; Published: 5 June 2020



Abstract: Photocatalysis by semiconductors is considered one of the most promising advanced oxidation processes (AOPs) and TiO₂ is the most well-studied material for the removal of contaminants from the aquatic system. Over the last 20 years, pharmaceuticals have been the most investigated pollutants. They re-enter the environment almost unmodified or slightly metabolized, especially in the aquatic environment, since the traditional urban wastewater treatment plants (WWTPs) are not able to abate them. Due to their continuous input, persistence in the environment, and unpleasant effects even at low concentrations, drugs are considered contaminants of emerging concern (ECs). Among these, we chose fluoroquinolone (FQ) antibiotics as an environmental probe for assessing the role of TiO₂ photocatalysis in the degradation of recalcitrant pollutants under environmental conditions and detoxification of surface waters and wastewaters. Due to their widespread diffusion, their presence in the list of the most persistent pollutants, and because they have been deeply investigated and their multiform photochemistry is well-known, they are able to supply rich information, both chemical and toxicological, on all key steps of the oxidative degradation process. The present review article explores, in a non-exhaustive way, the relationship among pollution, toxicity and remediation through titanium dioxide photocatalysis, with particular attention to the toxicological aspect. By using FQs as the probe, in depth indications about the different phases of the process were obtained, and the results reported in this paper may be useful in the improvement of large-scale applications of this technology, and—through generally valid methods—they could be deployed to other pharmaceuticals and emerging recalcitrant contaminants.

Keywords: TiO₂ photosensitized degradation of drugs; fluoroquinolones; antibacterial resistance; ecotoxic effects

1. Introduction

The amount of energy consistently reaching Earth in the form of solar light (1366 W m^{-2}) [1] largely overcomes any other form of available energy. Almost half of the intensity crosses the atmosphere and reaches the ground.

Plants have evolved with a system, chlorophyll photosynthesis, to extract energy from solar light and convert it into fuel. Man, on the other hand, was not able to directly use this energy (until recent years) and learned to exploit the surplus energy accumulated in plant tissues thriving during the modern era as a result of crude oil exploitation. Uncontrolled utilization of natural and non-renewable resources, on a human time-scale, is no longer sustainable, as suggested by many natural and economic indicators. Although mankind is slowly taking some steps ahead, it still has a lot to learn from plants on how to convert and store solar light effectively and efficiently. On the other hand, we have also

discovered, through photocatalysis, another powerful way to utilize solar light to help realize a cleaner and greener planet and enjoy a well-functioning circular economy.

Since at least three decades ago, semiconductor photocatalysis has become by far the most pursued topic in the photosensitization field of photochemistry, and several lines of research, from hydrogen generation through catalyst-mediated water splitting, as well as to more environmentally devoted applications, such as air purification and water depollution, have been taken up [2–6]. In particular, the irradiation of titania aqueous suspensions has been extensively applied as an advanced oxidation process (AOP) for the depollution and photo-detoxification of contaminated waters [2–8]; over the last twenty years, drugs have been the most investigated pollutants [9–16].

Due to their recalcitrant behavior in traditional wastewater treatment plants (WWTPs), drugs have been considered contaminants of emerging concern (EC) [17,18], and in the last years five of them have been included in the watch list of substances for Union-wide monitoring in the field of water policy (2008/105/EC, 2015/495/EU and 2018/840/EU [18,19]).

Recent data demonstrate that up to 80 pharmaceutical and personal care products are present and have been detected worldwide—at low but detectable range of nanograms up to micrograms per liter—in surface water, groundwater and wastewater effluents [18–22], as well as in soil and manure [23–27]. There is concern about the effects of the entry of these compounds into the environment, as their behavior and that of their degradation products are still largely unknown; potential chronic effects of long-term and low-level exposures on environmental organisms and on human health are suspected. Even trace concentrations could negatively affect non-target living organisms, interfere with the endocrine system [28], or lead to the development of allergenic responses [29] and could certainly cause increased bacterial resistance, as reported in several studies [30–34].

Among different groups of pharmaceuticals, antibiotics are of special concern, as they are administrated in large quantities to humans and animals to treat diseases and infections and at sub-therapeutic levels for prophylactic, metaphylactic and therapeutic purposes, and they are used as feed additives to promote growth in livestock. Antibiotics for human use end up in wastewater, originating from hospital and municipal emissions [19–21,31–36], whereas veterinary drugs are excreted by animals and are released in the manure [23–27]. For decades, liquid manure from livestock farming and sewage sludge from wastewater treatment plants has been applied to agriculture fields as a sustainable source of nutrients [37].

Furthermore, the emergency caused by the rising development and spread of resistant bacteria in the environment due to the continuous presence of antimicrobial residues in waters and soils has been officially recognized by the action plan against the rising threats from Antimicrobial Resistance (AMR) [19].

The removal of antibiotics and other pharmaceuticals, as well as their transformation products (TPs) from waters is essential both from the perspective of sending the reclaimed water to water bodies and to ensure recycling of a precious and depletable resource, as reported in detail in the “Strategic Approach” recently proposed by the European Commission (Brussels, 11 March 2019). The document also encourages “innovation,” where it can help to address the risks due to pharmaceuticals pollution and, at the same time, favor the circular economy [19].

Photocatalysis is advancing among AOPs, because in this case all of the “dirty” work is assigned to the “greenest” of reagents (solar light) [38,39]. It has the big advantage among other AOPs of involving no addition of chemicals, which would result, at least, in the formation of a spent oxidant [7,13,40,41]; it also avoids the safety issues inherent in the use of ionizing irradiations [41,42]. Furthermore, the catalyst is a solid and can be recovered and eventually reused, or it can be immobilized to facilitate recovery [7,38,43].

As reported above, TiO₂-assisted photocatalysis is a well-established ECs abatement technique. Over recent years, studies examined TiO₂ with regard to its electrochemical and solid-state properties, mechanistic investigation, and its applications. Using the literature and based on our previous experience in the field [44–46], we present a critical collection of the literature dealing with the

connection among pollution, toxicity, and remediation through titanium dioxide photocatalysis. For this purpose, we chose fluoroquinolone antibiotics (FQs) as an environmental probe to demonstrate the efficacy and the efficiency of TiO₂ photocatalysis both in the degradation of recalcitrant and emerging pollutants under real conditions (natural and wastewaters, UV-A and solar light) and its effect on environmental microorganisms.

Specifically, FQs were selected for the following reasons:

- (1) They absorb strongly in the UV-A region, and they are photochemically reactive [44,47];
- (2) they are very useful antibacterial agents and form the last class of antibiotics of large-scale use, particularly in highly developed countries. In the 1980s, molecules of this class were synthesized in Europe and the USA for human use, and about ten years later, as veterinary medicines. They show both a broad activity spectrum against Gram-positive and Gram-negative bacteria, excellent oral absorption, and are also used as a prophylactic in husbandry [48];
- (3) their occurrence in the environment has been widely assessed in past decades both in the aquatic and soil environment [18–27];
- (4) the strong stability of the quinolone ring slows down the degradation rate of these biotically resistant molecules. Toxicity is linked to the heteroaromatic ring, and thus is not fully abated in the first steps of the degradation [44–46];
- (5) the broad knowledge gathered around their photochemical reactivity, photoproducts, and photoreaction mechanism allows a clear separation of the catalyst effect from baseline photoreactivity.

2. Why We Used TiO₂ and Drugs as the Probe

Water remediation by means of irradiated titanium dioxide suspensions has become by far the most thoroughly investigated topic in the field of photocatalysis and photochemistry in general, with several journals virtually devoted to this topic and an increasing production of publications [2–9].

The sharp increase of papers published in the field is due to the solid evidence of the mechanism and the excellent properties of this material that has a minimal (photo)toxicity, good long-term stability, is low-cost and requires virtually no treatment prior to application. It is true that some increase in efficiency could be obtained either by using a single crystal phase (the commercial material is a mixture of anatase, rutile and brookite) [49–51], by controlling the micro-structure or the organization of the semiconductor [52], or through either metal or non-metal ion doping that allows fraction of solar energy absorbed toward the visible to be extended, although this reduces the potentially accessible range of oxidizable molecules [52,53]. The overall efficacy of these changes is still relatively limited and the first experiment carried out with commercial titania powder gives a satisfactory estimate of the final result [49].

The large presence of TiO₂ industrially available as a white pigment for paints, paper, food and other uses offers an inexpensive common basis that facilitates comparisons, often giving the best results directly when using the material in the commercial form (typically Evonik P25).

Even for less experienced researchers, titanium dioxide still remains the first choice and affords a common vocabulary for anybody interested in water depollution.

In principle, the irradiation of the TiO₂ photocatalyst with a light of energy greater than the bandgap of the semiconductor leads to the generation of a couple of positive holes (h^+) in the valence band and free electrons (e^-) in the conduction band.

Photo-induced charge separation on the catalyst surface may overcome electron cb/hole vb recombination (occurring in the ps to ns range) and leads to charge migration within the semiconductor/adsorbed molecule complex. Here, the electron transfer from the organic molecule, occurring at a rate from 10^8 to 10^{11} M⁻¹ s⁻¹, initiates a sequence of reactions that eventually end in complete mineralization, in the so-called process of “cold combustion”, which is mechanistically similar to the Fenton reaction. At the same time, photogenerated holes can react with water and generate a

powerful non-selective oxidant, the OH radical, which can effectively attack many organic compounds (Figure 1); on the other hand, photogenerated electrons, in the presence of dissolved oxygen, can form the superoxide anion and other strong oxidants species.

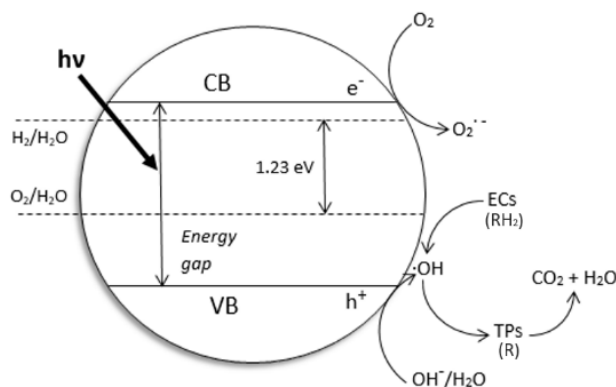


Figure 1. Mechanism of TiO₂ photocatalysis (ECs—contaminants of emerging concern, TPs—transformation products, VB—valence band, CB—conduction band).

The key steps here are the rates and equilibria of adsorption/desorption of both the parent compound and the reluctant intermediates on the semiconductor surface, and the complex sequence of competing reactions occurring at the semiconductor surface, especially in real matrices. A sequence of intertwined events takes place, each of them undergoing a specific effect, including back electron transfer, and resulting in a largely different efficiency (quantum yield, QY).

A detailed explanation of each of those mechanisms goes beyond the scope of this paper. Nonetheless, the overall process can be generalized in terms of the overall reaction, QY.

The overall photocatalytic QY of the process is influenced by several factors and competing effects occurring under the experimental conditions including, but not limited to, the fraction of light absorbed by the catalyst, the fraction of substrate adsorbed on the catalyst surface, and the rates of competing deactivation (both physical and chemical) reaction pathways.

The single contribution of all these processes to the photocatalytic reaction quantum efficiency often cannot be isolated and independently determined. While a number of overall reaction QYs has been determined for several systems, these are often not far from the QY \approx 0.1 value estimated by the initial workers, and no largely applicable rationalizations of the changes in QY are available as yet [54–57].

Dyes have been historically studied because of the easy and sensitive determination of their decomposition, but their use for quantitative measurement of photodegradation appears to be intrinsically a poor choice, especially in environmentally relevant conditions. Indeed, during dye irradiation, many side processes may occur, such as direct light absorption of the dye and sensitization of dissolved oxygen, and this may cause a large error in the evaluation of the process QY [58].

From a practical point of view, drugs are a far better choice in judging the efficiency and efficacy of TiO₂ photocatalysis as a means of water depollution and detoxification. In particular, the diversity of available structures has a large impact on their intrinsic photo-reactivity that can be carefully controlled, e.g., many drugs contain a (hetero)-cyclic moiety and thus absorb more light and give primary products that are also photo-reactive, because the aromatic ring is conserved until several steps occur, while the reverse holds for aliphatic drugs. From this perspective, FQs may become a gold standard. As light-driven reactivity is the only open route to FQs removal, this makes this class of antibiotics a perfect model to evaluate the efficacy of TiO₂ suspension in real conditions, that is, UV-A or sunlight, and natural and wastewater samples. The extensive knowledge of their physical properties and their peculiar photochemistry help in evaluating the contribution of each underlying

reaction mechanism to the overall degradation, thus isolating the purely TiO₂-mediated photocatalytic processes from all the other effects.

3. Fluoroquinolone Antibiotics

The two most investigated FQs are Ciprofloxacin (CIP) [59–64] and Ofloxacin (OFL) [59,62,64–69]. Other FQs include Enrofloxacin (ENR) [62], Levofloxacin (LEV) [70], Lomefloxacin (LOM) [59], Moxifloxacin (MOX) [71], and Norfloxacin (NOR) [62] (see Figure 2).

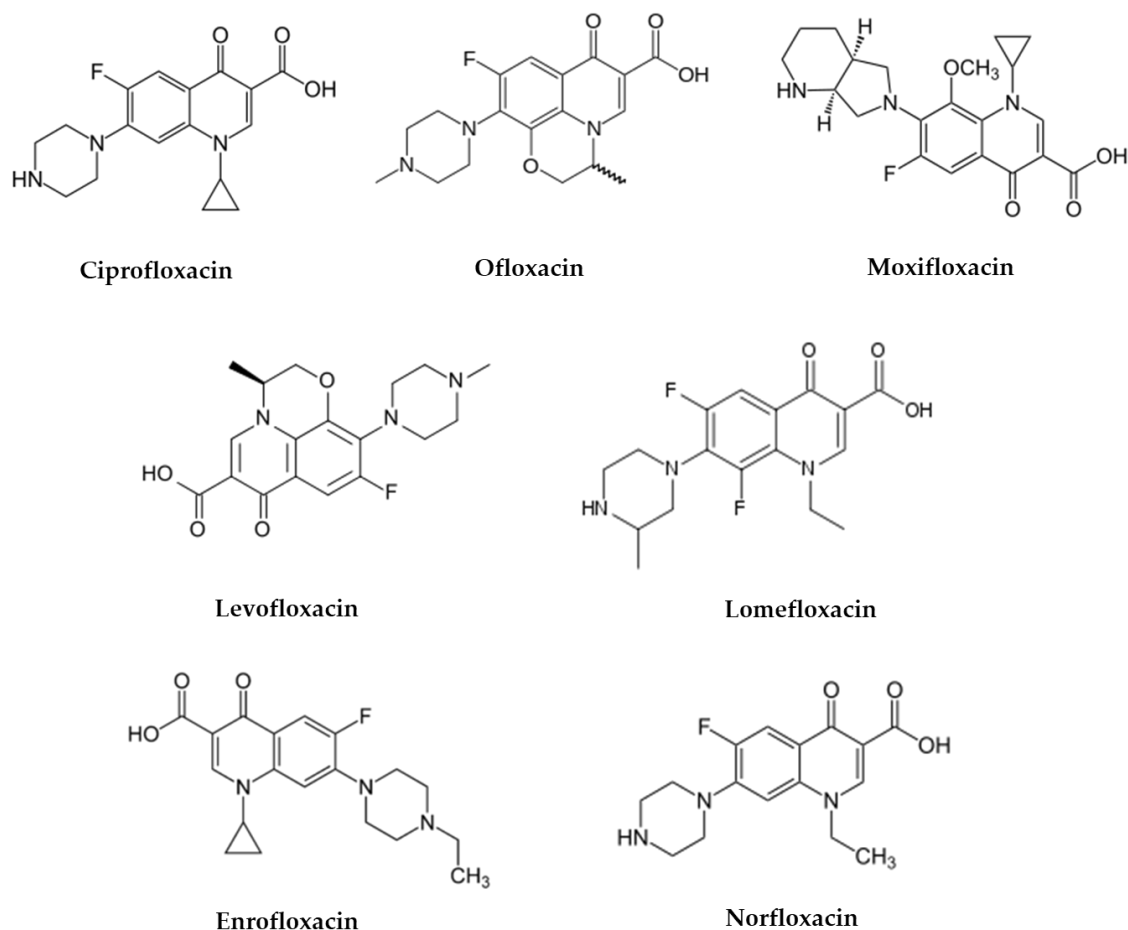


Figure 2. Chemical structures of the most investigated fluoroquinolones.

3.1. Fluoroquinolone Degradation Kinetics and Phototransformation Products

The oxidation process that occurs during the photocatalytic process involves five steps: (i) Diffusion of the reagent molecules from the bulk to the surface of the catalyst, (ii) adsorption of the reagent molecules on the catalyst surface, (iii) reaction on the surface and TPs formation, (iv) TPs desorption from the catalyst surface, and (v) TPs diffusion in bulk. The most common way to describe this process is the Langmuir–Hinshelwood (L–H) model (Equation (1)):

$$r = \frac{k_r \times K_{HL} \times C}{1 + K_{HL} \times C} \quad (1)$$

where C is the substrate concentration in the liquid phase after equilibrium, K_{HL} is the LH adsorption coefficient, k_r is the reaction rate coefficient, and r is the initial degradation rate.

For FQ concentrations ranging from tens of $\mu\text{g L}^{-1}$ to tens of mg L^{-1} , $K_{HL} \times C$ is much less than the unity, and the degradation rate can be simplified as follows:

$$r = -\frac{dC}{dt} = k_r \times K_{LH} \times C \cong k_{deg} \times C \quad (2)$$

All experimental data fit a pseudo-first-order equation:

$$\frac{C}{C_0} = e^{-k_{deg}t} \quad (3)$$

where C_0 is the initial substrate concentration, C is the substrate concentration at time t , and k_{deg} is the kinetic degradation constant.

Although many authors calculated the kinetic degradation constant (k_{deg}) through the common linear correlation between $\ln [C]/[C_0]$ and the irradiation time, giving undue weight to the first points of the curve, k_{deg} is a more convenient parameter to compare the photocatalytic performances of different systems, since it is independent of concentration. In Table 1, the kinetic degradation constant values are reported.

As shown in Table 1, TiO_2 Degussa P25 is used without modification [49,50]. Hombikat UV100 and PC500 were used by Paul et al. [63] and Venacio et al. [59] for comparison. Differing from P25, they displayed the sole crystallized anatase phase and a higher and microporous specific surface area of 330 and 290 $\text{m}^2 \text{g}^{-1}$, respectively [50,51,58]. Venancio et al. [59] synthesized highly crystalline TiO_2 nanoparticles with a high density through the sol-gel method. Despite the different morpho-structural characteristics, degradation rates were not significantly different from those obtained in the presence of TiO_2 P25.

The influence of different variables in the photo-oxidation process, such as the initial substrate concentration, amount of catalyst, solution pH, oxygen dissolved, temperature, oxidizing species, scavenger effects, and adsorption effects has been investigated by many research groups [59,60,62,65,67,68].

Concentrations of antibiotics in the range 10–50 mg L^{-1} were appropriately used to facilitate the identification of photodegradation products [60,62–64,67,68,70,71] and the accurate quantification of dissolved organic carbon (DOC) removal [60,64,67,68,71]—a few works were carried out at lower FQ concentrations (100–560 $\mu\text{g L}^{-1}$) [59,61,65,69] to better mimic actual conditions.

Ultrapure or deionized water was the most common solvent employed for the photochemical experiments [61–64,70,71]. It was chosen to avoid any possible interaction by a more complex matrix like surface water and wastewater. It is well known that the matrix constituents of both natural freshwaters and wastewaters may affect the photocatalytic process. Indeed, some inorganic ions and the fraction of natural dissolved organic matter (DOM) can act as photo-sensitizers able to absorb solar light directly [72]. As hinted above, in several cases, transient species are produced in the photosensitized degradation of FQs which exhibit an absorption spectrum similar to that of the starting material, as is normal since it is mostly determined by the heteroaromatic moiety, and may make the process somewhat more complex. It can further be observed that Venancio et al. [59] and Guzman et al. [60] showed that fluoroquinolone degradation occurred slower in natural waters than in ultrapure water; more precisely, the rate of degradation followed the order ultrapure water < simulated water < bottle water < tap water (see Figure 3).

Table 1. Exemplificative conditions of the photocatalytic degradation of fluoroquinolones and antibacterial and eco-toxicological tests.

FQ	Catalyst	Irradiation Source	Matrix	Model organism	Primary TPs/pathway	Abatement %	Ecotoxic effects	Ref.
[OFL] 100 µg L ⁻¹ mixed with other antibiotics	Evonik P25 (1 g L ⁻¹)	4 UV high-intensity LEDs 9 W, 15–515 W m ⁻²	Secondary treated effluent from urban WWTP pH = 7.2	<i>E. coli</i> , <i>Enterococcaceae</i> , heterotrophs	-	[OFL] < LOD in 15 min both actual and spiked samples with a variable antibiotic concentration Spiked: k_{deg} 0.290 min ⁻¹ Spiked (MeOH): k_{deg} 0.270 min ⁻¹	Bacterial activity inhibition: ≈ 2 log-units Bacteria regrowth after the treatment: similar (heterotrophs and <i>E. coli</i>) and lower (<i>Enterococcaceae</i>) than in the untreated sample	[65]
[CIP], [OFL], [LOM] 100 µg L ⁻¹	Evonik P25 (0.1 g L ⁻¹); PC500 (0.05 g L ⁻¹)	UV-A lamp, 8W	Ultrapure water; tap water pH = 7.0; commercial bottle water pH = 7.6; simulated water USEPA pH = 7.0	<i>E. coli</i> , <i>B. subtilis</i>	Primary TPs from attack on piperazine ring	95% FQs degraded in 120 min and after 60 min with saturated oxygen P25: k_{deg} 0.038–0.045 min ⁻¹ PC500: k_{deg} 0.035–0.050 min ⁻¹ Matrix effect: Ultrapure < simulated < bottle < tap water PC500 more efficient than P25	Bacterial activity reduced by 120 min PC500: 92% for <i>E. coli</i> , 78% for <i>B. subtilis</i> P25: 95% for <i>E. coli</i> , 84% for <i>B. subtilis</i> P25 more efficient than PC500	[59]
[CIP] 2–17 mg L ⁻¹	Evonik P25 (0.05 g L ⁻¹)	2 × 15 W lamps	Distilled water, mineral natural water pH = 6.4	<i>E. coli</i> , <i>S. aureus</i>	3 TPs, piperazine ring cleavage	100% CIP degraded in 350 min (ultrapure water) 90% CIP degraded in 500 min (mineral natural water) Matrix effect: ultrapure < mineral natural water	Bacterial activity differently reduced Distilled water: 85% for <i>S. aureus</i> , 50% for <i>E. coli</i> Mineral natural water: 80% for <i>S. aureus</i> , 45% for <i>E. coli</i> Different effects of TPs on bacteria strains	[60]
[CIP] 300 µg L ⁻¹	Evonik P25 (1 g L ⁻¹)	6 UV-A lamps 1.6–1.7 mW cm ⁻²	Ultrapure water	<i>V. fischeri</i>	7 TPs Degradation primarily on piperazine ring, defluorination	100% CIP degraded in less than 6 min	Slight toxicity after 15 min irradiation; higher toxicity (70%) after 45 min irradiation. Not excluded the contribution of irradiated TiO ₂ nanoparticles	[61]

Table 1. Cont.

FQ	Catalyst	Irradiation Source	Matrix	Model organism	Primary TPs/pathway	Abatement %	Ecotoxic effects	Ref.
[MOX] 50 mg L ⁻¹	Degussa P25 (1 g L ⁻¹)	UV-A pen ray 4 mW cm ⁻²	Phosphate buffer 10 mM pH = 7.0	<i>P. subcapitata</i>	13 TPs Core quinolone structure retained, no defluorination, transformation at R1 and R7. Presence of secondary TPs after MOX degradation	100% MOX degraded after 90 min	EC50 0.78 mg L ⁻¹ I% from 72% to 14% after 150 min treatment MOX contributes to growth inhibition more than its TPs	[71]
[LEV] 25 g L ⁻¹	TiO ₂ synthesized by a sol-gel method (1 g L ⁻¹)	7 × 18 W UV-A lamps 0.5 mW cm ⁻²	Distilled water	<i>E. coli</i>	-	90% LEV degraded in 120 min with home-made catalyst 78% and 80% LEV degraded in 120 min with P25 and PC50 Reusable catalyst	80% bacterial inhibition after 25 min irradiation 100% bacterial inhibition after 60 min irradiation	[70]
[OFL] 10 mg L ⁻¹	Aeroxide P25 (1 g L ⁻¹)	UV-A lamp 9W 3.16 W m ⁻²	Secondary treated effluent from urban WWTP pH = 8	<i>D. magna</i>	Major changes in N-piperazine ring Core quinolone structure retained, several competing pathways 20 TPs	US-UV-A-TiO ₂ : 100% OFL degraded, k_{deg} 0.105 min ⁻¹ UV-A-TiO ₂ : 85% OFL degraded, k_{deg} 0.073 min ⁻¹ slightly increasing in the presence of 0.14 mM H ₂ O ₂	TPs exhibit a long term toxicity (I% = 55, 60 min irradiation, 48 h exposure) Removal of toxic TPs after 240 min treatment	[67]
[OFL] 20 mg L ⁻¹	Aeroxide P25 (not specified)	UV-A medium pressure Hg lamp, 150 W	Mineral medium pH = 7.4	Closed bottle tests (OECD 301, 1992)	Opening of the piperazine ring, demethylation, decarboxylation	-	Primary TPs non-readily biodegradable; TPs persistence attributed to the fluorine	[66]
[OFL],[NOR],[CIP], [ENR] 10 mg L ⁻¹	Degussa P25 (0.5 g L ⁻¹)	Xenon lamp 800 W Simulated solar light irradiation	Deionized water pH = 6	<i>B. subtilis</i>	-	FQs 100% degraded in 90 min irradiation and in presence of 2.4 mM H ₂ O ₂ k_{deg} 0.022–0.027 min ⁻¹	Bacterial activity completely removed in 180 min irradiation FQs contribute to the antibacterial activity TPs do not exhibit a long term toxicity	[62]

Table 1. Cont.

FQ	Catalyst	Irradiation Source	Matrix	Model organism	Primary TPs/pathway	Abatement %	Ecotoxic effects	Ref.
[CIP] 33 mg L ⁻¹	Hombikat UV 100 (0.5 g L ⁻¹)	Xenon lamp 450 W UV-A, visible light 5.28 × 10 ⁻² –2.67 × 10 ⁻² W cm ⁻²	Deionized water pH = 6	<i>E. coli</i>	Piperazine ring cleavage Core quinolone structure retained	CIP 100% degraded in 30 min under UV-A/TiO ₂ CIP 90% degraded in 60 min under Vis/TiO ₂	Total CIP inactivation under laboratory conditions TPs retain negligible antibacterial activity	[63]
[OFL] 10 mg L ⁻¹	Degussa P25 (3 g L ⁻¹)	Xenon lamp 1 kW 272 W m ⁻² Simulated solar light irradiation	Secondary treated effluent from urban WWTP pH = 8	<i>D. magna</i>	Piperazine ring, FQ moiety	k_{deg} 0.009 min ⁻¹ , k_{deg} 0.016 min ⁻¹ (5.5 mM H ₂ O ₂)	OFL treated effluents relatively non-toxic (highest immobilization at 48 h of exposure)	[68]
[CIP], [OFL] 15 mg L ⁻¹	Degussa P25 (0.2 g L ⁻¹)	Xenon lamp 1500 W Simulated solar light irradiation	Deionized water	<i>V. fischeri</i>	CIP: piperazine moiety and quinolone moiety OFL: piperazine moiety and methyl groups, quinolone core unmodified	100% CIP and OFL degraded in 30 min	CIP and its TPs do not exhibit acute toxicity OFL TPs exhibit toxicity (I % = 55, 10 min irradiation, 15 min incubation)	[64]
[OFL] 560 µg L ⁻¹ mixed with other drugs	Degussa P25 (0.3 g L ⁻¹)	300W Simulated solar light irradiation	Moderately hard synthetic medium (MHW-EPA) pH = 7.6	<i>S. leopoliensis</i> , <i>B. calyciflorus</i>	-	80% mixture degraded both suspended and immobilized TiO ₂ in 48 h irradiation	9% bacterial inactivation with suspended TiO ₂ , no inactivation with supported TiO ₂ potentially toxic TPs	[69]

Fluoroquinolones (FQs), Transformation products (TPs), Ciprofloxacin (CIP), Ofloxacin (OFL), Enrofloxacin (ENR), Levofloxacin (LEV), Lomefloxacin (LOM), Moxifloxacin (MOX), Norfloxacin (NOR), kinetic degradation constant (k_{deg}), growth inhibition (I%), effective dose that causes 50% of the growth inhibition (EC50).

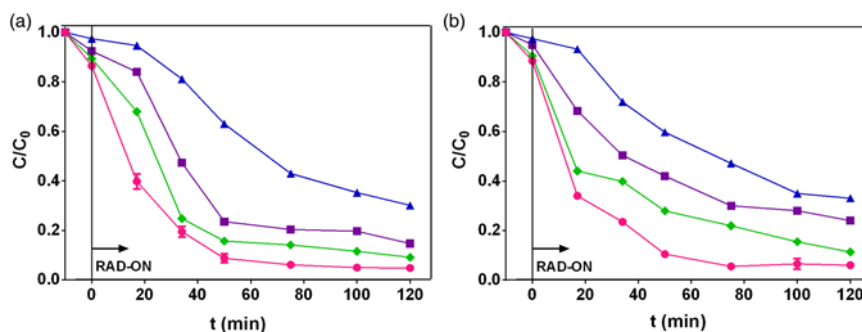


Figure 3. Ciprofloxacin degradation ($C_0 = 100 \mu\text{g L}^{-1}$) by (a) P25 (100 mg L^{-1}) and (b) PC500 (50 mg L^{-1}) in different water matrices. Ultrapure (●), simulated (◆), bottled (■) and tap water (▲). Reprinted with permission from [59], copyright 2018, IWA.

Similar, but more marked results were obtained by Hapeshi et al. [67] and Micheal et al. [68] in secondary treated effluent samples taken from an urban WWTP. Around 80% of OFL degraded after 120 min of irradiation.

Additionally, the pH of the solution affects the degradation of these antibiotics. The pH is correlated to both the intrinsic properties of the substrate and the surface charge density of the catalyst. It is reported that the adsorption of the organic compound, and thus its degradation, is favored near the zero point charge (zpc) of the catalyst. A medium pH may affect both the position of vb and cb and the band gap energy [65]. At pH 6, zpc of TiO₂ P25 is 6, and FQs are mainly in their cationic and zwitterion forms (half way between the pK_a of the acidic and the alkaline functional groups, see Figure 4). Adsorption experiments demonstrated that FQs adsorption, ensured by an appropriate stirring time in the dark, onto the surface catalyst was favored at pH values close to neutral.

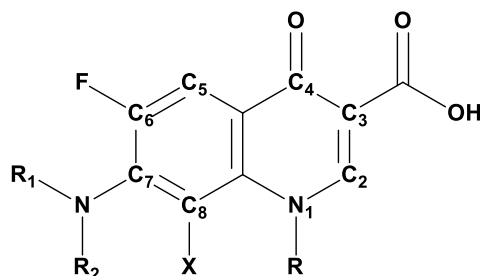


Figure 4. General fluoroquinolone (FQ) structure (X = H or F; carboxylic acid group, pK_{a1} , alkaline amine functional groups, pK_{a2}).

In neutral or slightly alkaline conditions, like those of natural freshwaters, hydroxyl radicals are more easily generated on the TiO₂ catalyst surface due to the oxidation of the adsorbed hydroxyl ions, and therefore the efficiency of the process is enhanced (see Figure 5) [62,67].

As expected, the photocatalytic efficiency is affected by the catalyst loading. Indeed, by increasing the catalyst amount, the number of available active sites increases; consequently, the substrate degradation rate rises. On the other hand, concentrations higher than some grams per liter may cause light scattering, poor light penetration or agglomeration phenomena in the suspension, which leads to a sharp drop in the substrate degradation rate [62,65,68].

Other experimental variables, in particular, temperature and oxygen percentage, seem to have minor relevance in the process efficiency. Specifically, Hapeshi et al. [67] observed that the degradation rate was enhanced by bubbling oxygen through the solution, especially in the first steps of the process, while only in the presence of a saturated working solution, fluoroquinolones were quantitatively abated in half the time, as reported by Venancio et al. [59].

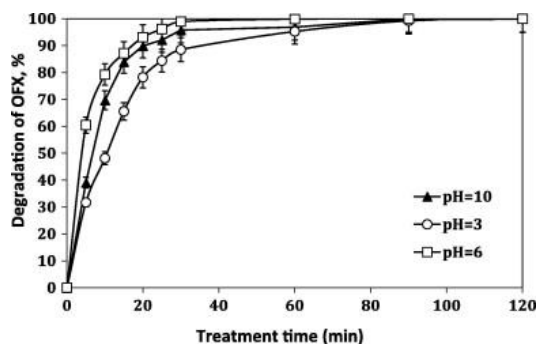


Figure 5. Effect of the pH solution on the degradation of Ofloxacin (OFX). Experimental conditions: $[OFX]_0 = 10 \text{ mg/L}$; $[TiO_2] = 1 \text{ g/L}$; 640 W/L. Reprinted with permission from [67], copyright 2013, Elsevier.

Micheal et al. [68] demonstrated that the effect of temperature had no significant impact on the conversion rate.

On the other hand, the addition of an oxidizing reagent, such as hydrogen peroxide, promotes both the oxidation process and total organic carbon (TOC) removal [62,67,68]. A slight increase in the degradation rate was observed, increasing H_2O_2 from 0.14 to 5.5 mM (see Table 1).

On the contrary, a decrease in the degradation rate was found by Biancullo et al. in the presence of a radical scavenger, such as MeOH (see Table 1) [65].

A comparison of the rates of degradation of CIP using different irradiation protocols revealed that UV-A/ TiO_2 photocatalysis was more efficient than Vis/ TiO_2 one, as shown by Paul et al. [63].

A higher kinetic degradation constant value, and consequently, a higher percentage of dissolved organic carbon, was obtained by using UV-A sonophotocatalytic treatment. Ultrasonic radiation applied by Hapeshi et al. [67] contributed to promoting the formation of reactive radicals, favored the substrate mass transfer from the bulk to the catalyst surface, and helped to avoid particle aggregation.

Biancullo et al. [65] obtained the highest k_{deg} value by using a UV-A irradiation LEDs system that was more efficient than the traditional lamps.

The identification and quantification of transformation products arising from photo-reactive molecules is a difficult task because no analytical standards are available for their identification and quantification; moreover, many different TPs may occur depending on the experimental and analytical setup [73]. Despite this limitation, TPs' evolution profiles are usually monitored, and chemical structures are proposed with an acceptable degree of certainty.

As for the photocatalytic degradation of FQs, many TPs were already present in the early steps of the process, with a lifetime usually in the same order as that of the starting molecule. On the contrary, the presence of secondary photoproducts was often confirmed by TOC measurements, which still indicated the presence of an organic load after the substrate degradation was complete en route to mineralization (see Figure 6) [60,64,67,68,71].

Generally, and in all the considered research papers, the chemical structures of TPs were based on high-resolution mass determination, and mechanistic pathways were quite accurately suggested. Unlike direct photolysis, in the presence of a photocatalyst, the oxidative degradation of the electron-rich amine side-chain results in the main chemical path followed by hydroxylation and decarboxylation, while photoproducts coming from direct photolysis, such as reductive dehalogenation and fluorine substitution, are not predominant as reported in most of the considered papers (see Scheme 1 and Table 1) [45].

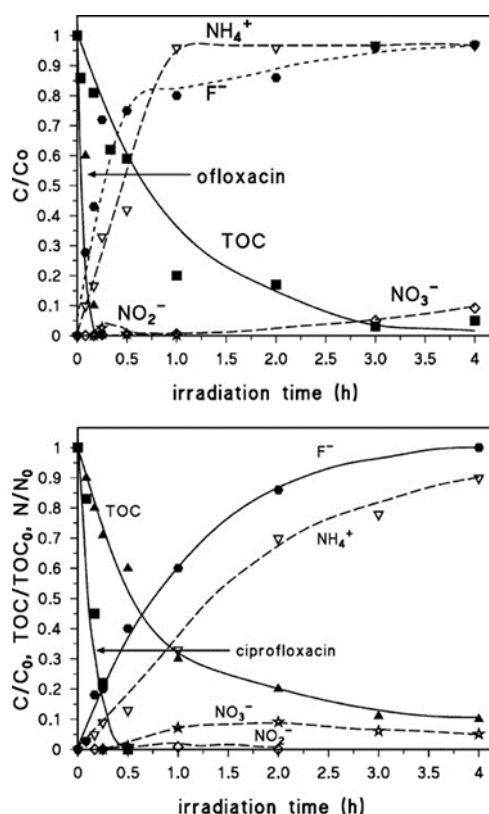
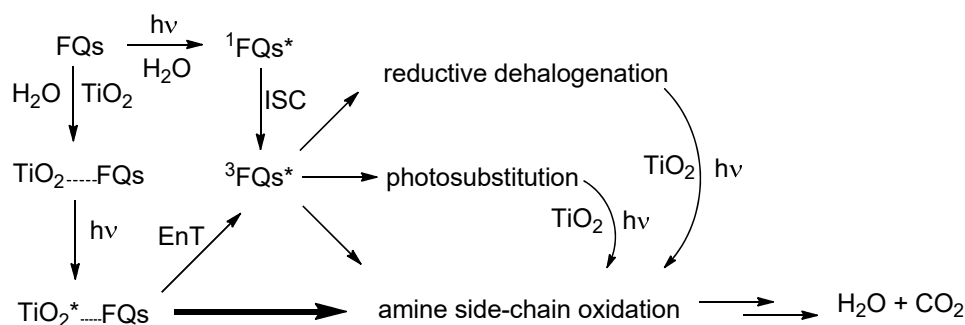


Figure 6. Degradation of ofloxacin (top) and ciprofloxacin (bottom) 15 mg L^{-1} on TiO_2 200 mg L^{-1} ; disappearance of initial compound, total organic carbon (TOC) and evolution of fluoride, ammonium, nitrite and nitrate ions. Reprinted with permission [64], copyright 2008, John Wiley and Sons.



Scheme 1. Photolytic and photocatalytic degradation paths for FQs.

At the experimentally reported TiO_2 concentrations, most of the light is absorbed by the titania particles, which then interact through hydrogen or electron transfer with the adsorbed drug [45,74,75]. Furthermore, FQ activation and degradation can also be initiated by energy transfer between photoactivated titania nanoparticles and FQs, producing a triplet of the latter, as reported in our previous works on Ofloxacin [76]. This mechanism accounts for the identification of low quantities of secondary products from direct photolysis.

Direct photolysis initiated photodegradation suffers from the limited part of the solar spectrum the FQs can absorb (usually below 380 nm for most FQs), which does not cover the visible part of the spectrum, and from the competitive light absorption of many other environmentally present organic compounds. Furthermore, the main photo-reaction paths for FQs are accessible only through their long-living triplet excited state; this transient must be populated through Inter System Crossing (ISC) from the first excited singlet and, once formed, may suffer from different deactivation pathways which can compete with photoreaction (i.e., electron transfer and energy transfer) especially under real

conditions where inorganic ions and organic compounds may easily foster these processes. When direct photolysis occurs, products from reductive dehalogenation and fluorine substitution dominate in the 6-FQs family, while the presence of a second fluorine atom at position 8, in addition, to increasing the photoreaction quantum yield, shifts the reactivity toward F elimination from C8. Unlike photolysis, during photocatalysis at the commonly employed concentrations, most of the light is absorbed by the semiconductor and not by the molecule used as the probe [74,75]. Furthermore, the TiO₂ UV-Vis absorption spectrum expands toward the visible region of light (400–410 nm, 3.0–3.2 eV), depending on the crystalline structure [77]. This allows for a better exploitation of sunlight radiation. In this case, after light absorption and electron-hole pair generation in the semiconductor, the FQ molecule adsorbed onto the catalyst surface reacts mostly through either direct or OH radical-mediated hydrogen and electron transfer [45]. This privileged reaction path in the presence of titanium dioxide photocatalyst massively increases the number of photoproducts originating from the oxidative degradation of the electron-rich FQs side-chains (Scheme 1 and Table 1). It ultimately initiates a cascade of reactions, eventually leading to complete mineralization and pollutant removal, with only water and carbon dioxide being released as by-products.

3.2. Antibacterial and Ecotoxicological Tests

As is apparent, TiO₂ is a strong photo-oxidant and has a bactericidal action towards a broad spectrum of harmful microorganisms [14,78,79]. For this reason, microbiological and eco-toxicological tests performed on irradiated samples are useful tools to evaluate the efficiency and the efficacy of the photocatalytic process, both in terms of degradation (decomposition degree of the target molecules) and detoxification (inactivation of the active principles, evaluation of acute and chronic effects against microorganisms). Nevertheless, testing the residual toxicity of toxic substances, such as pharmaceuticals, is a critical task, as sometimes the degradation TPs are more toxic than the parent compound, and at the same time it is impossible to isolate TPs. Due to the different experimental set ups, a significant variability among the obtained data was observed, although each test was performed following the standard guidelines [14,71].

In general, the experimental measurements allowed us to calculate the growth inhibition (I%) according to the following equation:

$$I\% = \frac{S_{control} - S_{sample}}{S_{control}} \times 100 \quad (4)$$

where $S_{control}$ is the signal measured in the control sample, and S_{sample} is the signal measured in the irradiated sample.

A dose–response curve may be obtained by plotting the I% calculated for each sample dilution against the log of the corresponding sample dilution. The log of the effective dose that causes 50% of the growth inhibition is reported as EC50.

An EC50 value against *P. subcapitata* was reported by Van Doorslaer et al. [71], who declared to have obtained the lowest value among those reported in the literature. It is apparent that by increasing the photocatalytic treatment, the inhibition decreases significantly, as shown by Paul et al. [63] (see Figure 7) and Venancio et al. [59], despite the different experimental conditions.

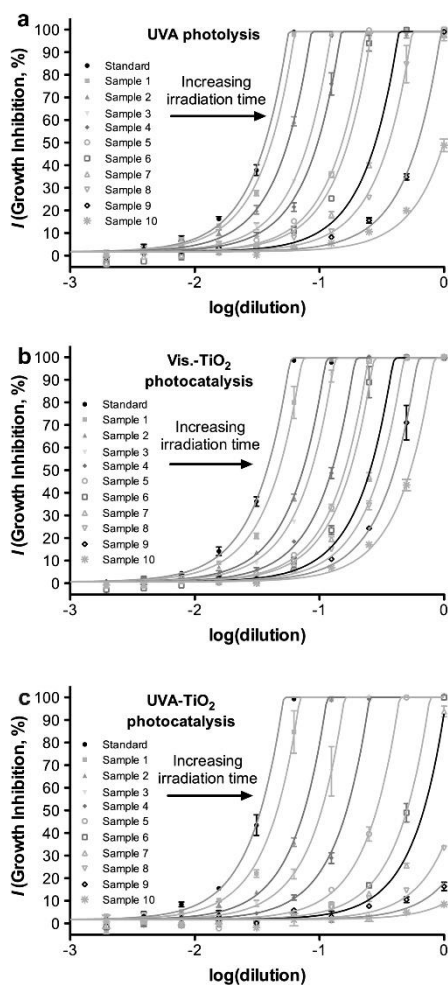


Figure 7. Dose–response relationships for deactivation of ciprofloxacin via (a) UV–A photolysis, (b) Vis- TiO_2 photocatalysis, and (c) UVA- TiO_2 photocatalysis in solutions initially dosed with 100 μM ciprofloxacin at pH 6, 25 $^\circ\text{C}$, and 0.5 g/L TiO_2 (for photocatalysis experiments). The averages of triplicate experimental measurements are shown with corresponding 95% confidence intervals. The independent variable “dilution” is equal to $1/2^n$, where “2” is the serial dilution factor used in preparing dose–response series (i.e., for two-fold, or 1:1 dilution), and “n” the number of times a given sample has been serially diluted relative to the corresponding parent sample (i.e., $1/2^0 = 1$ corresponds to the undiluted sample). Reprinted with permission from [63], copyright 2010, Elsevier.

Antibacterial and eco-toxicological tests used to evaluate changes in the residual antibacterial activity and the toxicity of FQs and their photoproducts are shown in Table 1.

Several organisms were used as a probe in the experiments, such as the microorganisms as *Bacillus subtilis* [59,62], *Staphylococcus aureus* [60] and *Escherichia coli* [59,60,63,65,70] collected from lab cultures, heterotrophic arthropods [65] and rotifers such as *Daphnia magna* [67,68] and *Brachionus calcyflorus* [69], algae (*Pseudokirchneriella subcapitata* [71], *Synechococcus. leopoliensis* [69]) and bacteria (*Enterococcaceae* [65], *Vibrio fischeri* [61,64]).

Van Dooslar et al. chose *P. subcapitata* as a model organism to evaluate the potential adverse effects occurring during MOX degradation [71]. They observed a significant increase of EC_{50} in the first hour of irradiation when the antibiotic was still present in the solution, while for longer irradiation times (90–150 min, $\text{MOX} < \text{LOD}$), the growth inhibition decreased from 72% to 14%. The residual toxicity and the poor carbon mineralization compared with the parent compound conversion confirmed the presence of TPs. Their lower toxicity may be ascribable either to a decrease of biological activity or to a minor permeation through the cell membrane due to their larger hydrophilicity compared to MOX.

A UV-A sonophotocatalytic treatment of OFL aqueous solutions against *D. magna* was carried out by Hapeshi et al. [67]. OFL was quickly consumed after 30 min of treatment leading to the formation of 20 TPs, while *D. magna* immobilization increased from 20% to 55% after 24 h and 48 h of exposure, respectively. A decrease in daphnid immobilization up to 5% was observed after 240 min of treatment, when TPs were removed.

Similar, but less marked results were obtained during the UV-A photocatalytic treatment of OFL, carried out under both the same experimental conditions [67] and in other work [68] in the presence of 3 g L^{-1} TiO_2 . In both cases, incomplete mineralization (around 10%) was observed after the antibiotic degradation confirmed the presence of toxic intermediates and daphnid immobilization up to 25% at a long-term exposure. The long-term toxicity was due to the formation of photoproducts that maintain the core quinolone structure.

Calza et al. [64] reported a reduction in the natural emission of the luminescent bacteria *V. fischeri* within the first 10 min of the OFL photolytic treatment, corresponding to a 55% inhibition after only 15 min of incubation. The simultaneous disappearance of the parent compound and the occurrence of TPs indicated that the toxicity was strictly correlated to TPs, especially when they retain the quinolone core structure. From 15 to 120 min of irradiation, the percentage inhibition decreased and TOC was almost completely abated (85%). An inhibition percentage below 1% and complete mineralization of the organic carbon was obtained after four hours of treatment (see Figure 8).

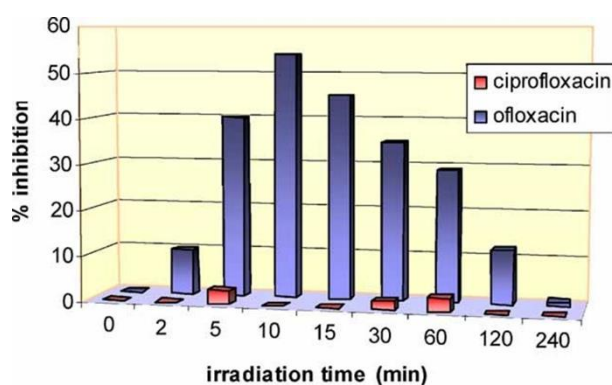


Figure 8. Inhibition (%) of the luminescence of bacteria *Vibrio fischeri* as a function of the photocatalytic treatment time for ofloxacin and ciprofloxacin. Reprinted with permission from [64], copyright 2008, John Wiley and Sons.

The *V. fischeri* bioassay was also adopted to investigate the eco-toxicological effects of CIP photodegradation [61,64]. For Calza et al. [64], CIP aqueous solutions tested at different irradiation times (2–240 min) were non-toxic, indicating that CIP degradation proceeded through the formation of non-toxic TPs, even if more than four hours of irradiation were necessary to obtain a 100% TOC abatement (see Figure 8).

In contrast, higher toxicity (70%) against *V. fischeri* in more diluted CIP solutions and for long irradiation time (45 min) was observed by Silva et al. [61], who did not exclude that irradiation in the presence of titanium dioxide may lead to toxic effects.

In good agreement with Calza's results, Paul et al. [63] demonstrated that for each mole of CIP degraded, the antimicrobial load (*E. coli*) in the irradiated solution decreased by a "mole", indicating that TPs retained a negligible antibacterial activity compared to the parent compound. The stoichiometric release of ammonium and fluoride ions confirmed quantitative CIP abatement, which was achieved faster under UV-A TiO_2 than Vis- TiO_2 .

Comparable findings were reported by Guzman et al. [60] both in distilled and mineral waters. CIP-irradiated samples (95% degradation, mineralization not exceeding 35%) were less harmful than non-irradiated samples, even if Gram-positive bacteria (*S. aureus*) seemed more vulnerable than the

Gram-negative bacteria (*E. coli*) to the main TPs (by about two-fold), which conserved the quinolone ring but not the amino-side chain.

Only three papers among those examined investigated the biological activity of the sole parent compound [59,62,70].

Venancio et al. [59] assessed the residual CIP, LOM, and OFL antibacterial activity against Gram-positive (*B. subtilis*) and Gram-negative (*E. coli*) strains during TiO₂ P25 and PC500 photocatalytic treatment. TiO₂ P25 removed almost the total antibacterial activity in a shorter reaction time (120 min of irradiation) compared to PC500.

Similar results were obtained by Li et al. [62]. An inhibition of 50% of the initial *E. coli* activity was reached after 120 min of irradiation with concentrated solutions of CIP, ENR, NOR, OFL. Although mineralization required a longer irradiation time than FQs degradation, biological activity was removed within 180 min.

A total of 90 min of treatment on the LEV solution in the presence of a TiO₂ homemade catalyst was enough to inhibit *E. coli* resistance completely [70].

Only two studies analyzed the photocatalytic degradation of a mixture of pharmaceuticals in effluents from urban WWTPs [65,69]. Today, urban WWTPs are considered a hot-spot for antibiotic-resistant bacteria proliferation, and clear data on the adverse toxic effects due to pharmaceuticals at actual concentrations on simple living organisms are still lacking.

Preliminary results were proposed by Andreozzi et al. [69]. They carried out toxicity tests exposing blue-green algae and a rotifer to an irradiated moderately hard synthetic aqueous sample containing OFL and other five pharmaceuticals at a concentration of hundredths of nanograms per liter.

The solutions were irradiated for 48h in the presence of either suspended or immobilized TiO₂. A slight reduction (9%) in the initial bioactivity was observed in the catalyst suspension, while supported TiO₂ nanoparticles on a membrane were less efficient than suspended nanoparticles. Based on the poor results obtained, the authors suppose that the presence of toxic TPs formed during the photocatalytic treatment.

Additional information was recently reported in a novel disinfection study by means of UV-A LEDs system applied to different WWTP samples collected on different days before and after spiking with a few hundredths of nanograms per liter of a mixture of antibiotics [65]. Interestingly, the count of various bacterial groups (heterotrophs, *E. coli*, and *Enterococcaceae*) was carried out both after the photocatalytic treatment and after three days of storage in the dark at room temperature. Although one-hour UV-A LED-irradiation was enough to inhibit the bacterial activity (about two log-units), a significant regrowth was observed after three days of storage. Specifically, the antibiotic resistance after treatment was similar to that of non-treated WWTP samples for heterotrophs and *E. coli* and lower for *Enterococcaceae* (see Figure 9). This phenomenon, not yet completely investigated, may be attributed to organic matter produced during the oxidative process. As is evident, actual matrices can play an important role not only in the photodegradation of recalcitrant molecules, but also in the photo-detoxification process.

Lastly, Vasquez et al. [66] described a 28 day biodegradability test where the microbiological conditions of the aqueous environment were simulated following the OECD guidelines. They evaluated the potential biodegradability of OFL and its transformation products formed during both the photocatalytic treatment and biotransformation processes. Although OFL was degraded quickly, mineralization remained low (6%), and the biodegradability value was negligible (around zero). These results indicated that primary TPs were not readily biodegradable, especially when fluorine was still present on the heteroaromatic ring.

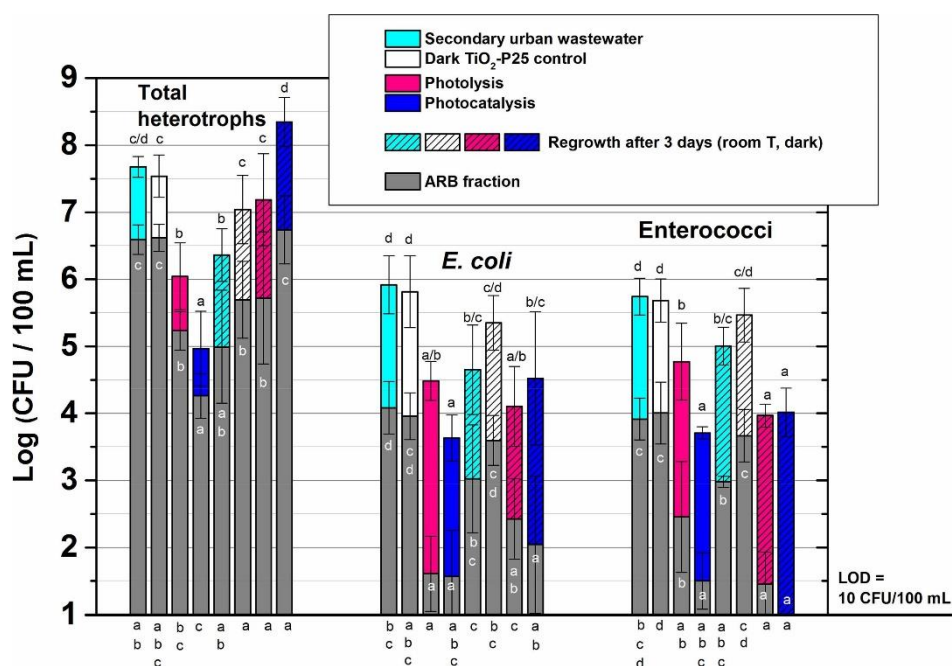


Figure 9. Total (colored) and antibiotic resistant (grey) bacteria inactivation after 1 h photolysis/ photocatalysis evaluated immediately (filled bars) and after three days of storage in the dark at room temperature (striped bars). The letters a, b, c, d, and e indicate significantly ($p < 0.05$) different groups among the tested treatment conditions. The letters in black on the top of bars refer to total bacteria. The letters in white refer to the antibiotic resistant counterparts. The letters on the bottom of the graph refer to the percentage of resistant bacteria with respect to the total bacteria. Reprinted with permission from [65], copyright 2019, Elsevier.

4. Conclusions on Benefits and Drawbacks

The widespread diffusion of drugs and pharmaceutical active compounds in the environment, especially in the aquatic compartment, is a matter of serious concern, since these are not abated by traditional urban WWTPs.

This review suggested, through the exploitation of results obtained with an appropriate model molecule (FQ), that TiO₂ photocatalysis may be considered as an efficient and convenient advanced oxidation process for the removal of pharmaceuticals from contaminated waters. Specifically, it may be considered one of the best advanced oxidation processes, being a safe and effective mineralization of the pollutants that requires no addition of chemicals, except the semiconductor, and may take place under natural sunlight. As opposed to simple photolysis, TiO₂ photocatalytic treatment is efficient in removing the harmful effects due to the presence of drug residues and TPs in the aquatic environment.

The detailed knowledge about the photo-reactivity of FQs and toxicity of their photoproducts offers a useful model both for predicting the effectiveness of the photocatalytic treatment against other persistent compounds and for rationalizing the behavior of new composite materials. Nevertheless, in our opinion, many key aspects still require some attention.

Although laboratory experiments allowed for an almost complete mineralization of pharmaceuticals and a complete reduction of the residual antibacterial activity, an absolute validity and a direct cross-reading for other persistent contaminants must be evaluated, especially in terms of their ecotoxicological effects. Furthermore, a full validation of this method to large-scale application and exhaustive case models are still missing.

The generated photoproducts, easy to recognize at the laboratory scale due to their higher concentrations and controlled experimental conditions, are difficult to determine in the presence of a matrix of environmental constituents, as well their additive, synergistic, or antagonist effects in the

presence of a mixture of contaminants. This point must be carefully taken into consideration during the identification of proper assays for the determination of the efficacy of TiO₂ AOP in real cases.

Problems related to the losses of catalyst in the environment, and its post-treatment separation and recovery cannot be ignored and must be accounted for. Nonetheless, the versatility of TiO₂ and deep knowledge of its properties, supported by many years of scientific studies, open the door to further technological improvements, such as immobilization and magnetic recovery, which certainly will take this powerful AOP towards widespread application in the near future.

Author Contributions: Conceptualization M.S., L.P., A.A., F.M., Writing—original draft M.S., L.P., A.A., Writing—review & editing M.S., L.P., F.M., Investigation (research literature) M.S., F.M., L.P., Visualization (figure design) A.C. All authors have read and agreed to the published version of the manuscript.

Funding: This research received no external funding

Conflicts of Interest: The authors declare no conflict of interest.

References

1. Available online: <https://www.britannica.com/science/solar-constant> (accessed on 22 April 2020).
2. Dionysiou, D.D.; Li Puma, G.; Jinhua Ye, J.; Jenny Schneider, J.; Bahnemann, D. *Photocatalysis: Applications*; RSC Publishing: Cambridge, UK, 2016.
3. Hernández-Ramírez, A.; Medina-Ramírez, I. *Photocatalytic Semiconductors. Synthesis, Characterization, and Environmental Applications*; Springer: Cham, Switzerland, 2015. [CrossRef]
4. Pichat, P. A brief survey of the practicality of using photocatalysis to purify the ambient air (indoors or outdoors) or air effluents. *Appl. Catal. B Environ.* **2019**, *245*, 770–776. [CrossRef]
5. Bahnemann, D.W.; Cunningham, J.; Fox, M.A.; Pelizzetti, E.; Pichat, P.; Serpone, N. Photocatalytic Treatment of Waters. In *Aquatic and Surface Photochemistry*, 1st ed.; Helz, R.G., Ed.; CRC Press: Boca Raton, FL, USA, 1994; pp. 261–316. [CrossRef]
6. Guillard, C.; Amalric, L.; D'Oliveira, J.C.; Delprat, H.; Hoang-Van, C.; Pichat, P. Heterogeneous photocatalysis: Use in water treatment and involvement in atmospheric chemistry. In *Aquatic and Surface Photochemistry*, 1st ed.; Helz, R.G., Ed.; CRC Press: Boca Raton, FL, USA, 2018. [CrossRef]
7. Serpone, N.; Horikoshi, S. Can the photocatalyst TiO₂ be incorporated into a wastewater treatment method? Background and prospects. *Catal. Today* **2020**, *340*, 334–346. [CrossRef]
8. Fagan, R.; McCormack, D.E.; Dionysiou, D.D.; Pillai, S.C. A review of solar and visible light active TiO₂ photocatalysis for treating bacteria, cyanotoxins and contaminants of emerging concern. *Mater. Sci. Semicond. Process* **2016**, *42*, 2–14. [CrossRef]
9. Kanakaraju, D.; Glass, B.D.; Oelgemöller, M. Titanium dioxide photocatalysis for pharmaceutical wastewater treatment. *Environ. Chem. Lett.* **2014**, *12*, 27–47. [CrossRef]
10. Etacheri, V.; Di Valentin, C.; Schneider, J.; Bahnemann, D.; Pillai, S.C. Visible-light activation of TiO₂ photocatalysts: Advances in theory and experiments. *J. Photochem. Photobiol. C* **2015**, *25*, 1–29. [CrossRef]
11. Kanakaraju, D.; Glass, B.D.; Oelgemöller, M. Advanced oxidation process-mediated removal of pharmaceuticals from water: A review. *J. Environ. Manag.* **2018**, *219*, 189–207. [CrossRef] [PubMed]
12. Albini, A.; Chen, C.; Sturini, M. Use the drugs and respect the environment. *Curr. Opin. Green Sustain. Chem.* **2017**, *6*, A1–A4. [CrossRef]
13. Nick Serpone, N.; Artemev, Y.M.; Ryabchuk, V.K.; Emeline, A.V.; Horikoshi, S. Light-driven advanced oxidation processes in the disposal of emerging pharmaceutical contaminants in aqueous media: A brief review. *Curr. Opin. Green Sustain. Chem.* **2017**, *6*, 18–33. [CrossRef]
14. Mahmoud, W.M.M.; Rastogi, T.; Kümmerer, K. Application of titanium dioxide nanoparticles as a photocatalyst for the removal of micropollutants such as pharmaceuticals from water. *Curr. Opin. Green Sustain. Chem.* **2017**, *6*, 1–10. [CrossRef]
15. Calvete, M.J.F.; Piccirillo, G.; Vinagreiro, C.S.; Pereira, M.M. Hybrid materials for heterogeneous photocatalytic degradation of antibiotics. *Coordin. Chem. Rev.* **2019**, *395*, 63–85. [CrossRef]
16. Babić, S.; Ćurković, L.; Ljubas, D.; Čizmić, M. TiO₂ assisted photocatalytic degradation of macrolide antibiotics. *Curr. Opin. Green Sustain. Chem.* **2017**, *6*, 34–41. [CrossRef]

17. Sauv e, S.; Desrosiers, M. A review of what is an emerging contaminant. *Chem. Central J.* **2014**, *8*, 15–21. [[CrossRef](#)]
18. Sousa, J.C.G.; Ribeiro, A.R.; Barbosa, M.O.; Fernando, M.; Pereira, R.; Silva, A.M.T. A review on environmental monitoring of water organic pollutants identified by EU guidelines. *J. Hazard. Mater.* **2018**, *344*, 146–162. [[CrossRef](#)] [[PubMed](#)]
19. European Union Strategic Approach to Pharmaceuticals in the Environment. Communication from the Commission to the European Parliament, the Council and the European Economic and Social Committee. Available online: <https://ec.europa.eu/transparency/regdoc/rep/1/2019/EN/COM-2019-128-F1-EN-MAIN-PART-1.PDF> (accessed on 22 October 2019).
20. Yang, Y.; Ok, Y.S.; Kim, K.H.; Kwon, E.E.; Tsang, Y.F. Occurrences and removal of pharmaceuticals and personal care products (PPCPs) in drinking water and water/sewage treatment plants: A review. *Sci. Total Environ.* **2017**, *596–597*, 303–320. [[CrossRef](#)] [[PubMed](#)]
21. Castiglioni, S.; Davoli, E.; Riva, F.; Palmiotto, M.; Camporini, P.; Manenti, A.; Zuccato, E. Data on occurrence and fate of emerging contaminants in a urbanized area. *Data Brief* **2018**, *17*, 533–543. [[CrossRef](#)] [[PubMed](#)]
22. Riva, F.; Castiglioni, S.; Fattore, E.; Manenti, A.; Davoli, E.; Zuccato, E. Monitoring in the drinking water of Milan and assessment of the human risk. *Int. J. Environ. Health* **2018**, *221*, 451–457. [[CrossRef](#)] [[PubMed](#)]
23. Ezzariai, A.; Hafidi, M.; Khadra, A.; Aemig, Q.; El Fels, L.; Barret, M.; Merlina, G.; Patureau, D.; Pinelli, E. Human and veterinary antibiotics during composting of sludge or manure: Global perspectives on persistence, degradation, and resistance genes. *J. Hazard. Mater.* **2018**, *359*, 465–481. [[CrossRef](#)] [[PubMed](#)]
24. Wei, R.; Ge, F.; Zhang, L.; Hou, X.; Cao, Y.; Gong, L.; Chen, M.; Wang, R.; Bao, E. Occurrence of 13 veterinary drugs in animal manure-amended soils in Eastern China. *Chemosphere* **2016**, *144*, 2377–2383. [[CrossRef](#)]
25. Quaik, S.; Embrandiri, A.; Ravindran, B.; Hossain, K.; Al Dhabi, N.A.; Arasu, M.V.; Ignacimuthu, S.; Ismail, N. Veterinary antibiotics in animal manure and manure laden soil: Scenario and challenges in Asian countries. *J. King Saud Univ. Sci.* **2020**, *32*, 1300–1305. [[CrossRef](#)]
26. Golet, E.M.; Strehler, A.; Alder, A.C.; Giger, W. Determination of fluoroquinolone antibacterial agents in sewage sludge and sludge-treated soil using accelerated solvent extraction followed by solid-phase extraction. *Anal. Chem.* **2002**, *74*, 5455–5462. [[CrossRef](#)]
27. Hu, X.; Luo, Y.; Zhou, Q. Simultaneous analysis of selected typical antibiotics in manure by microwave-assisted extraction and LC–MS. *Chromatographia* **2010**, *71*, 217–223. [[CrossRef](#)]
28. Adeel, M.; Song, X.; Wang, Y.; Francis, D.; Yang, Y. Environmental impact of estrogens on human, animal and plant life: A critical review. *Environ. Int.* **2017**, *99*, 107–119. [[CrossRef](#)] [[PubMed](#)]
29. Galbiati, V.; Papale, A.; Kummer, E.; Corsini, E. In vitro models to evaluate drug-induced hypersensitivity: Potential test based on activation of dendritic cells. *Front. Pharmacol.* **2016**, *7*, 204–214. [[CrossRef](#)] [[PubMed](#)]
30. Theuretzbacher, U. Global antibacterial resistance: The never-ending story. *J. Glob. Antimicrob. Resist.* **2013**, *1*, 63–69. [[CrossRef](#)] [[PubMed](#)]
31. Menz, J.; Baginska, E.; Arrhenius,  .; Hai , A.; Backhaus, T.; K mmerer, K. Antimicrobial activity of pharmaceutical cocktails in sewage treatment plant effluent—An experimental and predictive approach to mixture risk assessment. *Environ. Pollut.* **2017**, *231*, 1507–1517. [[CrossRef](#)] [[PubMed](#)]
32. K mmerer, K. Resistance in the environment. *J. Antimicrob. Chemother.* **2004**, *54*, 311–320. [[CrossRef](#)]
33. Lindberg, R.H.; Bj rklund, K.; Rendhal, P.; Johansson, M.I.; Tysklind, M.; Andersson, B.A.V. Environmental risk assessment of antibiotics in the Swedish environment with emphasis on sewage treatment plants. *Water Res.* **2007**, *41*, 613–619. [[CrossRef](#)]
34. Rodriguez-Mozaz, S.; Chamorro, S.; Marti, E.; Huerta, B.; Gros, M.; S nchez-Melsi , A.; Borrego, C.M.; Barcel , D.; Balc zar, J.L. Occurrence of antibiotics and antibiotic resistance genes in hospital and urban wastewaters and their impact on the receiving river. *Water Res.* **2015**, *69*, 234–242. [[CrossRef](#)]
35. Santos, L.H.M.L.M.; Gros, M.; Rodriguez-Mozaz, S.; Delerue-Matos, C.; Pena, A.; Barcel , D.; Montenegro, M.C.B.S.M. Contribution of hospital effluents to the load of pharmaceuticals in urban wastewaters: Identification of ecologically relevant pharmaceuticals. *Sci. Total Environ.* **2013**, *461–462*, 302–316. [[CrossRef](#)]
36. Verlicchi, P.; Galletti, A.; Petrovic, M.; Barcel , D. Hospital effluents as a source of emerging pollutants: An overview of micropollutants and sustainable treatment options. *J. Hydrol.* **2010**, *389*, 416–428. [[CrossRef](#)]
37. Mantovi, P.; Baldoni, G.; Toderi, G. Reuse of liquid, dewatered, and composted sewage sludge on agricultural land: Effects of long-term application on soil and crop. *Water Res.* **2005**, *39*, 286–296. [[CrossRef](#)] [[PubMed](#)]

38. Malato, S.; Fernández-Ibáñez, P.; Maldonado, M.I.; Blanco, J.; Gernjak, W. Decontamination and disinfection of water by solar photocatalysis: Recent overview and trends. *Catal. Today* **2009**, *147*, 1–59. [[CrossRef](#)]
39. Di Li, D.; Shi, W. Recent developments in visible-light photocatalytic degradation of antibiotics. *Chin. J. Catal.* **2016**, *37*, 792–799. [[CrossRef](#)]
40. Choi, H.; Al-Abed, S.R.; Dionysiou, D.D.; Stathatos, E.; Lianos, P. Chapter 8 TiO₂-based advanced oxidation nanotechnologies for water purification and reuse. *Sustain. Sci. Eng.* **2010**, *2*, 229–254. [[CrossRef](#)]
41. Wang, J.; Zhuang, R. Degradation of antibiotics by advanced oxidation processes: An overview. *Sci. Total Environ.* **2020**, *701*, 135023–135038. [[CrossRef](#)] [[PubMed](#)]
42. Esposito, B.R.; Capobianco, M.L.; Martelli, A.; Navacchia, M.L.; Pretali, L.; Saracino, M.; Zanelli, A.; Emmi, S.S. Advanced water remediation from ofloxacin by ionizing radiation. *Radiat. Phys. Chem.* **2017**, *141*, 118–124. [[CrossRef](#)]
43. Durán, A.; Monteagudo, J.M.; San Martín, I. Operation costs of the solar photo-catalytic degradation of pharmaceuticals in water: A mini-review. *Chemosphere* **2018**, *211*, 482–488. [[CrossRef](#)]
44. Sturini, M.; Speltini, A.; Maraschi, F.; Profumo, A.; Pretali, L.; Irastorza, E.A.; Fasani, E.; Albini, A. Photolytic and photocatalytic degradation of fluoroquinolones in untreated river water under natural sunlight. *Appl. Catal. B Environ.* **2012**, *32*, 119–120. [[CrossRef](#)]
45. Sturini, M.; Speltini, A.; Maraschi, F.; Pretali, L.; Ferri, E.N.; Profumo, A. Sunlight-induced degradation of fluoroquinolones in wastewater effluent: Photoproducts identification and toxicity. *Chemosphere* **2015**, *134*, 313–318. [[CrossRef](#)]
46. Sturini, M.; Speltini, A.; Maraschi, F.; Pretali, L.; Profumo, A.; Fasani, E.; Albini, A.; Migliavacca, R.; Nucleo, E. Photodegradation of fluoroquinolones in surface water and antimicrobial activity of the photoproducts. *Water. Res.* **2012**, *46*, 5575–5582. [[CrossRef](#)]
47. Albini, A.; Monti, S. Photophysics and photochemistry of fluoroquinolones. *Chem. Soc. Rev.* **2003**, *32*, 238–250. [[CrossRef](#)] [[PubMed](#)]
48. Thu, D.M.; Pham, T.D.M.; Ziora, Z.M.; Blaskovich, M.A.T. Quinolone antibiotics. *Med. Chem. Commun.* **2019**, *10*, 1719–1739. [[CrossRef](#)]
49. Hurum, D.C.; Agrios, A.G.; Gray, K.A.; Rajh, T.; Thurnauer, M.C. Explaining the Enhanced Photocatalytic Activity of Degussa P25 Mixed-Phase TiO₂ Using EPR. *J. Phys. Chem. B* **2003**, *107*, 4545–4549. [[CrossRef](#)]
50. Ohtani, B.; Prieto-Mahaney, O.O.; Li, D.; Abe, R. What is Degussa (Evonik) P25? Crystalline composition analysis, reconstruction from isolated pure particles and photocatalytic activities. *J. Photochem. Photobiol. A Chem.* **2010**, *216*, 179–182. [[CrossRef](#)]
51. Alonso-Tellez, A.; Masson, R.; Robert, D.; Keller, N.; Keller, V. Comparison of Hombikat UV100 and P25 TiO₂ performance in gas-phase photocatalytic oxidation reaction. *Chemistry* **2012**, *250*, 58–65. [[CrossRef](#)]
52. Reddy, P.A.K.; Reddy, P.V.L.; Kwon, E.; Kim, K.-H.; Akter, T.; Kalagara, S. Recent advances in photocatalytic treatment of pollutants in aqueous media. *Environ. Int.* **2016**, *91*, 94–103. [[CrossRef](#)]
53. Sturini, M.; Maraschi, F.; Cantalupi, A.; Pretali, L.; Nicolis, S.; Dondi, D.; Profumo, A.; Caratto, V.; Sanguineti, E.; Ferretti, M.; et al. TiO₂ and N-TiO₂ Sepiolite and Zeolite Composites for Photocatalytic Removal of Ofloxacin from Polluted Water. *Materials* **2020**, *13*, 537. [[CrossRef](#)]
54. Sun, L.; Bolton, J.R. Determination of the Quantum Yield for the photochemical generation of hydroxyl radicals in TiO₂ suspensions. *J. Phys. Chem.* **1996**, *100*, 4127–4134. [[CrossRef](#)]
55. Serpone, N.; Salinaro, A. Terminology, relative photonic efficiencies and quantum yields in heterogeneous photocatalysis. Part I: Suggested protocol. *Pure Appl. Chem.* **1999**, *71*, 303–320. [[CrossRef](#)]
56. Salinaro, A.; Emeline, A.V.; Zhao, J.; Hidaka, H.; Ryabchuk, V.K.; Serpone, N. Terminology, relative photonic efficiencies and quantum yields in heterogeneous photocatalysis. Part II: Experimental determination of quantum yields. *Pure Appl. Chem.* **1999**, *71*, 321–335. [[CrossRef](#)]
57. Kisch, H. On the problem of comparing rates or apparent quantum yields in heterogeneous photocatalysis. *Angew. Chem. Int. Ed.* **2010**, *49*, 9588–9589. [[CrossRef](#)] [[PubMed](#)]
58. Barbero, N.; Vione, D. Why Dyes should not be used to test the photocatalytic activity of semiconductor oxides. *Environ. Sci. Technol.* **2016**, *50*, 2130–2131. [[CrossRef](#)] [[PubMed](#)]
59. Venancio, W.A.L.; Rodrigues-Silva, C.; Maniero, M.G.; Guimarães Lima, J.R. Photocatalytic removal of fluoroquinolones and their antimicrobial activity from water matrices at trace levels: A comparison of commercial TiO₂ catalysts. *Water Sci. Technol.* **2018**, *78*, 1668–1678. [[CrossRef](#)]

60. Villegas-Guzman, P.; Oppenheimer-Barrot, S.; Silva-Agredo, J.; Torres-Palma, R.A. Comparative Evaluation of Photo-Chemical AOPs for Ciprofloxacin degradation: Elimination in natural waters and analysis of pH effect, primary degradation by-products, and the relationship with the antibiotic activity. *Water Air Soil Pollut.* **2017**, *228*, 209–224. [[CrossRef](#)]
61. Silva, A.R.; Martins, P.M.; Teixeira, S.; Carabineiro, S.A.C.; Kuehn, K.; Cuniberti, G.; Alves, M.M.; Lanceros-Mendezag, S.; Pereira, L. Ciprofloxacin wastewater treated by UVA photocatalysis: Contribution of irradiated TiO₂ and ZnO nanoparticles on the final toxicity as assessed by *Vibrio fischeri*. *RSC Adv.* **2016**, *6*, 95494–95503. [[CrossRef](#)]
62. Li, W.; Guo, C.; Su, B.; Xu, J. Photodegradation of four fluoroquinolone compounds by titanium dioxide under simulated solar light irradiation. *J. Chem. Technol. Biotechnol.* **2012**, *87*, 643–650. [[CrossRef](#)]
63. Paul, T.; Dodd, M.C.; Strathmann, T.J. Photolytic and photocatalytic decomposition of aqueous ciprofloxacin: Transformation products and residual antibacterial activity. *Water Res.* **2010**, *44*, 3121–3132. [[CrossRef](#)]
64. Calza, P.; Medana, C.; Carbone, F.; Giancotti, V.; Baiocchi, C. Characterization of intermediate compounds formed upon photoinduced degradation of quinolones by high performance liquid chromatography/high-resolution multiple-stage mass spectrometry. *Rapid Commun. Mass Spectrom.* **2008**, *22*, 1533–1552. [[CrossRef](#)]
65. Biancullo, F.; Moreira, N.F.F.; Ribeiro, A.R.; Manaia, C.M.; Faria, J.L.; Nunes, O.C.; Castro-Silva, S.M.; Silva, A.M.T. Heterogeneous photocatalysis using UVA-LEDs for the removal of antibiotics and antibiotic resistant bacteria from urban wastewater treatment plant effluents. *Chem. Eng. J.* **2019**, *367*, 304–313. [[CrossRef](#)]
66. Vasquez, M.I.; Hapeshi, E.; Fatta-Kassinos, D.; Kümmerer, K. Biodegradation potential of ofloxacin and its resulting transformation products during photolytic and photocatalytic treatment. *Environ. Sci. Pollut. Res.* **2013**, *20*, 1302–1309. [[CrossRef](#)]
67. Hapeshi, E.; Fotiou, I.; Fatta-Kassinos, D. Sonophotocatalytic treatment of ofloxacin in secondary treated effluent and elucidation of its transformation products. *Chem. Eng. J.* **2013**, *224*, 96–105. [[CrossRef](#)]
68. Michael, I.; Hapeshi, E.; Michael, C.; Fatta-Kassinos, D. Solar Fenton and solar TiO₂ catalytic treatment of ofloxacin in secondary treated effluents: Evaluation of operational and kinetic parameters. *Water Res.* **2010**, *44*, 5450–5462. [[CrossRef](#)]
69. Andreozzi, R.; Campanella, L.; Frayse, B.; Garric, J.; Gonnella, A.; Lo Giudice, R.; Marotta, R.; Pinto, G.; Pollio, A. Effects of advanced oxidation processes (AOPs) on the toxicity of a mixture of pharmaceuticals. *Water Sci. Technol.* **2004**, *50*, 23–28. [[CrossRef](#)]
70. Sushil Kumar Kansal, S.K.; Kundu, P.; Sood, S.; Lamba, R.; Umar, A.; Mehta, S.K. Photocatalytic degradation of the antibiotic levofloxacin using highly crystalline TiO₂ nanoparticles. *New J. Chem.* **2014**, *38*, 3220–3226. [[CrossRef](#)]
71. Van Doorslaer, X.; Haylamicheal, I.D.; Dewulf, J.; Van Langenhove, H.; Janssen, C.R.; Demeestere, K. Heterogeneous photocatalysis of moxifloxacin in water: Chemical transformation and ecotoxicity. *Chemosphere* **2015**, *119*, S75–S80. [[CrossRef](#)]
72. Vione, D.; Scozzaro, A. Photochemistry of surface fresh waters in the framework of climate change. *Environ. Sci. Technol.* **2019**, *53*, 7945–7963. [[CrossRef](#)]
73. Jimenez-Villarín, J.; Serra-Clusellas, A.; Martínez, C.; Conesa, A.; Garcia-Montaña, J.; Moyano, E. Liquid chromatography coupled to tandem and high resolution mass spectrometry for the characterisation of ofloxacin transformation products after titanium dioxide photocatalysis. *J. Chromatogr. A* **2016**, *1443*, 201–210. [[CrossRef](#)]
74. Paul, T.; Miller, P.L.; Strathmann, T.J. Visible-light-mediated TiO₂ photocatalysis of fluoroquinolone antibacterial agents. *Environ. Sci. Technol.* **2007**, *41*, 4720–4727. [[CrossRef](#)]
75. Van Doorslaer, X.; Heynderickx, P.M.; Demeestere, K.; Debevere, K.; Van Langenhove, H.; Dewulf, J. UV-A and UV-C induced photolytic and photocatalytic degradation of aqueous ciprofloxacin and moxifloxacin: Reaction kinetics and role of adsorption. *Appl. Catal. B Environ.* **2011**, *101*, 540–547. [[CrossRef](#)]
76. Sturini, M.; Speltini, A.; Maraschi, F.; Vinci, G.; Profumo, A.; Pretali, L.; Albini, A.; Malavasi, L. g-C₃N₄-promoted degradation of ofloxacin antibiotic in natural waters under simulated sunlight. *Environ. Sci. Pollut. Res.* **2017**, *24*, 4153–4161. [[CrossRef](#)]
77. Ola, O.; Maroto-Valer, M.M. Review of material design and reactor engineering on TiO₂ photocatalysis for CO₂ reduction. *J. Photochem. Photobiol. C Photochem. Rev.* **2015**, *24*, 16–42. [[CrossRef](#)]

78. Ziental, D.; Czarczynska-Goslinska, B.; Mlynarczyk, D.T.; Glowacka-Sobotta, A.; Stanisz, B.; Goslinski, T.; Sobotta, L. Titanium dioxide nanoparticles: Prospects and applications in medicine. *Nanomaterials* **2020**, *10*, 387. [[CrossRef](#)] [[PubMed](#)]
79. Hoseinzadeh, E.; Makhdoumi, P.; Taha, P.; Hossini, H.; Stelling, J.; Kamal, M.A.; Ashraf, G.M. A review on nano-antimicrobials: Metal nanoparticles, methods and mechanisms. *Curr. Drug Metab.* **2017**, *18*, 120–128. [[CrossRef](#)]



© 2020 by the authors. Licensee MDPI, Basel, Switzerland. This article is an open access article distributed under the terms and conditions of the Creative Commons Attribution (CC BY) license (<http://creativecommons.org/licenses/by/4.0/>).